CHEMMEDCHEM

CHEMISTRY ENABLING DRUG DISCOVERY

Accepted Article

Title: Inhibitors against Fungal Cell Wall-remodelling Enzymes

Authors: Pedro Merino, Ignacio Delso, Jessika Valero-Gonzalez, Fernando Gomollon-Bel, Jorge Castro-Lopez, Wenxia Fang, Iva Navratilova, Daan M. F. van Aalten, Tomas Tejero, and Ramon Hurtado-Guerrero

To be cited as: *ChemMedChem* 10.1002/cmdc.201700720

Link to VoR: http://dx.doi.org/10.1002/cmdc.201700720

A Journal of

ChemPubSoc Europe

WILEY-VCH

www.chemmedchem.org

10.1002/cmdc.201700720
WILEY-VCH

COMMUNICATION

Inhibitors against Fungal Cell Wall-remodelling Enzymes.

Ignacio Delso,*[a] Jessika Valero-Gonzalez,[b] Fernando Gomollón-Bel,[a] Jorge Castro-López,[b] Wenxia Fang,[c] Iva Navratilova,[c] Daan M.F. van Aalten,[c] Tomás Tejero,[a] Pedro Merino,*[b] and Ramon Hurtado-Guerrero*[b,d]

Abstract: Fungal β-1,3-glucan glucanosyltransferases are glucan-remodeling enzymes that play important roles in cell wall integrity, and are essential for the viability of pathogenic fungi/yeasts. As such, they are considered possible drug targets, although inhibitors of this class of enzymes have not yet been reported. Here, we report a multidisciplinary approach, based on a structure-guided design using a highly conserved transglycosylase from *Sacharomyces cerevisiae*, that leads to carbohydrate derivatives with high affinity for *Aspergillus fumigatus* Gel4. We demonstrate by X-ray crystallo-graphy that the compounds bind in the active site of Gas2/Gel4 and interact with the catalytic machinery. The topological analysis of non-covalent interactions demonstrates that the combination of a triazole with positively charged aromatic moieties are important for optimal interactions with Gas2/Gel4 through unusual pyridinium cation-π and face-to-face π-π interactions. The lead compound is capable of inhibiting *Af*Gel4 with an IC_{50} value of 42 μM.

The fungal cell wall is essential for the integrity of the cell, providing strength, shape and protection against environmental insults.[1] However, rather than being a rigid structure it has inherent plasticity during cell growth and adaptation to the environment.[2] Cell wall remodelling enzymes and in particular the large family of β-1,3-glucan glucanosyltransferases or transglycosylases (TGs) contribute to this plasticity.[3] These enzymes remodel the polysaccharide β-1,3-glucan, which is the major component of the fungal cell wall. They cleave the β-1,3 bond of β-1,3-glucan oligosaccharides with at least 10 glucose units and transfer the newly formed reducing end (>5 glucose units) to the nonreducing end of another β-1,3-glucan oligosaccharide, resulting in the elongation of the β-1,3-glucan.[4] These TGs have been found in all fungal species investigated to date and are named differently depending on the fungi or yeasts in which they are found (e.g. Gelp, Gasp and Phrp in *A. fumigatus*, *S. cerevisiae* and *C. albicans*, respectively).[5] In yeasts, these TGs have important roles in spore and hyphal wall assembly, and maintaining cell wall integrity during vegetative growth, and are essential for viability of *Schizosaccharomyces pombe*.[6] In fungi, the gene encoding the TG Gel4 in *A. fumigatus* is also essential for viability.[4] This family of TGs is grouped into 3 subfamilies based on the presence or absence of CBM43, a carbohydrate binding module most commonly associated with β(1-3)glucan binding activity and a serine/threonine-rich region that contains *O*-glycosylation putative sites.[4,7] We previously reported the crystal structure of *Sc*Gas2 in complex with laminarioligossacharides[7] and recently trapped a covalent intermediate on the pathway to transglycoslation (Figure 1).[8] From these structures, we defined the different sites for the sugar moieties bound in the donor and acceptor sites, and we also verified the role of the proposed acid-base Glu176 and the nucleophile Glu275.

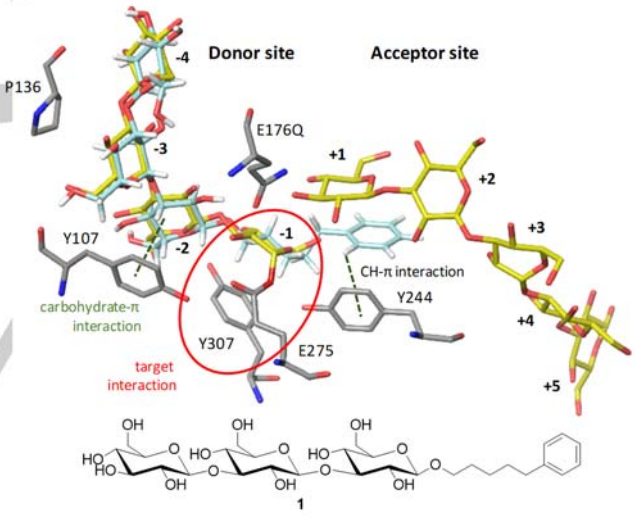

Figure 1. View of the active site of the covalent intermediate of E176Q *Sc*Gas2 with laminaritetraose (donor site) in complex with laminaripentaose (acceptor site; see PDB ID: 5FIH [ref]). The carbons of the oligosaccharides are shown as yellow sticks. Compound **1** (carbons shown as cyan sticks) docked in *Sc*Gas2 active site is superposed with the above structure. Residues as grey sticks are involved in interactions with the sugar moieties and compound **1.** Note that laminaritetraose is covalently bound to E275.

Although these enzymes are potential antifungal drug targets, there are currently no potent inhibitors of this family of enzymes. We previously synthetized[9] and characterised compound **1**, a laminaritriose derivative bound to a phenyl moiety through a flexible linker, which showed a poor affinity (K_d = 800 ± 100 μM) towards Gas2 (Figure 1). We used *Sc*Gas2 for our studies here because it is a homologue of *Af*Gel4, a proposed antifungal drug target, and its crystal structure has been reported.[7] *Sc*Gas2 is

[a] Dr. I. Delso, Dr. F. Gomollón-Bel and Prof. T. Tejero
Instituto de Síntesis Química y Catálisis Homogénea (ISQCH). Universidad de Zaragoza. CSIC. E-50009 Zaragoza. Aragón, Spain.
E-mail: idelso@unizar.es
[b] Dr. J. Valero-González, J. Castro-López, Dr. R. Hurtado-Guerrero and Prof. P. Merino
Institute of Biocomputation and Physics of Complex Systems (BIFI), University of Zaragoza. BIFI-IQFR (CSIC) Joint Unit, Campus Rio Ebro. E-mail: rhurtado@bifi.es; E-mail: pmerino@unizar.es
[c] Dr. W. Fang, Dr. I. Navratilova, and Prof. D.M.F. van Aalten; Centre for Gene Regulation and Expression, School of Life Sciences, University of Dundee, Dundee DD1 5EH, Scotland
[d] Fundación ARAID, 50018, Zaragoza, Spain.

10.1002/cmdc.201700720

similar to *Af*Gel4 at the sequence level (ca. 50% sequence identity in the catalytic domains, and 100% if considering all the key residues recognising carbohydrates from -3 to +1; see Figure S1).[7] The rationale for making compound **1** was to occupy the donor site with the sugar moieties by interacting with the conserved Pro136 and Tyr107, and reach the acceptor site establishing CH-pi interactions between the phenyl moiety and the conserved Tyr244, as exemplified by a docked model of compound **1** in the *Sc*Gas2 active site (Figure 1). In this model, the trisaccharide moiety occupies the -2 to -4 subsites and two conserved tyrosine residues (Tyr107 and Tyr244) interact with the sugar unit occupying position -1 (carbohydrate-π interactions)[10] and the phenyl group of at the ligand tail (CH-π interactions).[11] Taking advantage of the high structural homology and the complete conservation of the active site among *Af*Gel4 and *Sc*Gas2, we reasoned that the introduction of an additional aromatic moiety interacting an additional conserved tyrosine (Tyr307, Figure 1) could result in an enhanced binding for both *Af*Gel4 and *Sc*Gas2. Simultaneously, it should also be possible to explore different aromatic residues at the ligand tail to enhance interactions with Tyr244.

In this study, we explore the use of a triazole scaffold to reach Tyr307 taking advantage of two amenable and efficient synthetic strategies based on click chemistry.[12] We demonstrate the strength of this strategy by synthesizing eleven different candidates and determining their dissociation constants (K_ds) towards *Sc*Gas2 and *Af*Gel4. The results demonstrate that the laminaritriose moiety directly bound to a triazole together with positively charged aromatic moieties at ligand tail are important for an optimal interaction with these enzymes. The observed results are confirmed by solving the crystal structures of *Sc*Gas2 in complex with 7 out of the 11 compounds by X-ray crystallography studies in combination with computational NCI analyses. These data also show that hydrophobic interactions, particularly π-π and azinium-π (cation-π) interactions, between Tyr244 and the aromatic moieties at the ligand tail, as well as between the triazole moiety and Tyr307, are the determinants of the increased affinity for *Sc*Gas2.

Introduction of the triazole ring into the linker was achieved through the well-known CuAAC reaction applied to carbohydrate chemistry (Scheme 1).[13] Two alternative coupling strategies for preparing the triazole ring were explored, i.e.: laminarioligosaccharide alkyne with a properly substituted azide and laminarioligosaccharide azides[[4] with properly substituted alkynes. Compound **2**, an analogue of compound **1** containing a triazole ring in the linker, was prepared following the first strategy. However, docking studies with **2** (Glide, see SI) showed that the triazole ring did not reach the target Tyr307. In fact, with *Sc*Gas2 we obtained a value of K_d = 17.0 ± 0.1 μM for **2** (Table 1, entry 2), higher than the K_d for the equivalent compound **6**, which differed in the position of the triazole (K_d = 6.2 ± 0.1 μM; see below for its synthesis).

Docking studies suggested that a triazole positioned closer to the sugar units as well as electron-poor aromatic residues at the ligand tail would increase the affinity of the ligand (See SI). Consequently, we prepared compounds **3-12** following the strategy illustrated in Scheme 1. In order to evaluate the effect in binding of the carbohydrate units we also prepared mono- (**3-4**) and disaccharides (**5**) in addition to potential ligands bearing a trisaccharide unit. Monosaccharides **3-4** and disaccharide **5** showed high K_d values, reinforcing our finding that three units of trisaccharide are required as a minimum recognition scaffold.

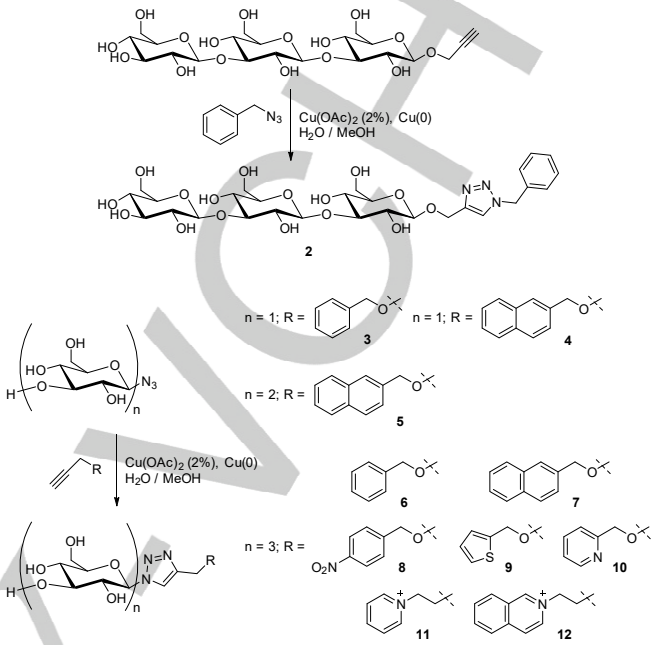

Scheme 1. Chemical synthesis of ligands through typical click-chemistry.

Table 1. Dissociation constants of compounds **1**-**12** for *Sc*Gas2 and *Af*Gel4.

entry	**Compound**	K_d (*Sc*Gas2) (μM)	K_d (*Af*Gel4) (μM)
1	**1**[a]	800 ± 100	nd[b]
2	**2**	17 ± 0.1	nd
3	**3**	171 ± 1	nd
4	**4**	72 ± 1	nd
5	**5**	68 ± 1	nd
6	**6**	6.2 ± 0.1	6.00 ± 0.06
7	**7**	13.00 ± 0.01	10.0 ± 0.1
8	**8**	9.80 ± 0.07	nd
9	**9**	4.09 ± 0.04	3.60 ± 0.03
10	**10**	8.06 ± 0.07	5.30 ± 0.06
11	**11**	4.60 ± 0.03	2.50 ± 0.02
12	**12**	3.10 ± 0.02	1.50 ± 0.01

[a] = determined by tryptophan fluorescence spectroscopy; [b] nd = not determined. Laminaritriose showed too weak affinity to be measured.

Aromatic residues in compounds **6** and **7** lowered the K_d values for *Sc*Gas2, similar values being observed for *Af*Gel4 in line with a high identity between enzymes. Increasing of the size

ring from phenyl (**6**) to naphthyl (**7**) did not improve binding affinity. Employing an electron withdrawing substituent on the aromatic ring we observed an intermediate value and with the thienyl-derivative **9** (Table 1, entry 9), we obtained one of the lowest K_d values observed for both *Sc*Gas2 and *Af*Gel4. In searching for stronger π-π interactions by introducing π-deficient aromatic rings which can interact in a more efficient way[15] with the electron rich aromatic ring of tyrosine, we moved to the pyridine derivative **10** which, at physiological pK_a is amenable to be protonated to some extent as demonstrated by NMR experiments (see SI). Moderate K_d values were obtained for both enzymes (Table 1, entry 10). Using positively charged pyridinium moiety as in **11** (Table 1, entry 11) reduced the K_d, particularly for *Af*Gel4, which was further enhanced when we moved from pyridinium **11** to quinolinium derivative **12** (Table 1, entry 12). Compound **12** showed K_d = 3.10 ± 0.02 and 1.50 ± 0.01 μM, against *Sc*Gas2 and *Af*Gel4, respectively, being the lowest found among all the prepared glycomimetics. Figure 2 illustrates determination of the K_d for compound **12** towards *Sc*Gas2 by SPR. In addition, we could not obtain a K_d for laminaritriose due to its low affinity. This result points to the introduced groups (triazole ring and aromatic residues) as the responsible of the tight binding of the designed glycomimetics to both enzymes.

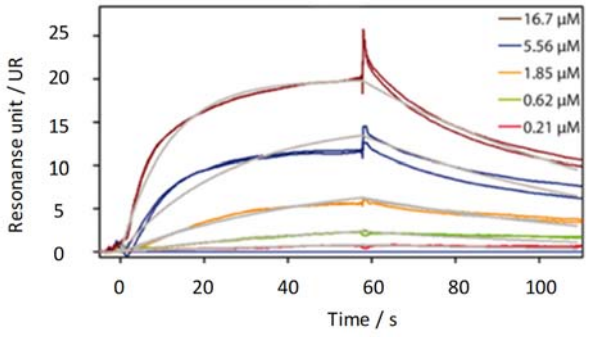

Figure 2. Surface plasmon resonance (SPR) measurements for compound **12** towards *Sc*Gas2. The various concentrations of **12** show the binding reaction and the calculated dissociation constant is 3.1 ± 0.02 μM. Plain brown lines show the fitted curve of non-linear regression.

To elucidate the binding mode of the designed glycomimetics we solved the crystal structures of compounds **6**-**12** in complex with *Sc*Gas2 at high resolution, ranging from 1.4 to 2.15 Å (Figure 4, ESI). In all cases, the trisaccharide unit occupied the donor site in the -2, -3 and -4 positions. The triazole ring was observed to form π-π stacking interactions with Y307. The observed interactions of the aromatic residue located at the ligand tail were different depending on the ring type. Thus, whereas ligands **6**-**9** adopt a T-shape (edge-to-face) orientation of the aromatic residues with respect to Tyr244, positively charged residues in **11** and **12** adopt a parallel orientation. The case of pyridine derivative **10** deserves a more detailed discussion.

In addition, for compounds **6**, **8** and **9**, another ligand molecule is observed at the acceptor site, likely due to the less optimal interactions between the radical at the tail position with Y244 (see Figure S2). The observed T-shape orientation observed for compounds **6**-**9** corresponds to a typical CH-π interaction, as that observed in the docked structure of **1**. In the case of compound **10,** two conformations were found in the X-ray structure (Figure 3, E). One conformation corresponds to the neutral ligand folded on itself and stabilized by intramolecular π-π interactions with the thiazole ring and H-bonding with a water molecule, which is also interacting with E176 and E275. Notably, the other conformation corresponds to a protonated pyridine ring, which adopts a parallel orientation with respect to Tyr244. This favours a transfer of charge between the Tyr244 electron-rich aromatic ring and the electron-poor pyridinium ring through pyridinium−π (cation−π) interaction, which has been shown to be stronger than the typical face-to-face π−π interactions,[16] rarely observed in protein structures where most of the orientations are T-shaped (also named as edge-to-face).[17]

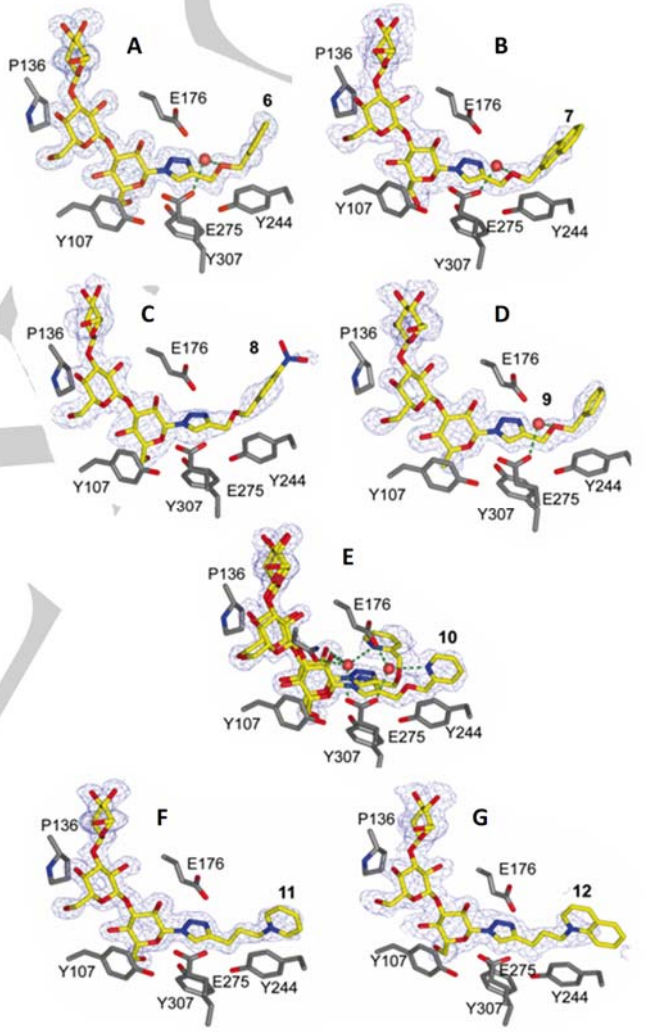

Figure 3. X-ray structures of *Sc*Gas2 in complex with **6** (A), **7** (B), **8** (C), **9** (D), **10** (E), **11** (F) and **12** (G). The unbiased (i.e. before inclusion of any ligand model) $|F_o|$- $|F_c|$, ϕ_{calc} electron density maps are shown at 2.2 σ.

To evaluate the conformational preferences, we carried out a molecular dynamics (MD) study of *Sc*Gas2 in complex with compound **10** in folded/unfolded and protonated/neutral states (Figure 4). MD calculations showed that both protonated and neutral folded derivatives become unfolded after 0.6 and 2.5 ns, respectively. This result suggests that the unfolded conformation is the most representative. The results observed with compound **10** indicate that the presence of a positively charged π-deficient

aromatic residue induces a change of the relative orientation between the aromatic residue and Tyr244. Indeed, when the positive charge is permanent (at physiological pH) as in the case of aziniums **11** and **12**, only unfolded conformations with a parallel orientation to Tyr244 are found in the X-ray structure. The parallel orientation allows more efficient π,π-interactions with Tyr244 in comparison with CH-π interactions observed in compounds **6-9**. The existence of these interactions was confirmed through a topological NCI analysis[18] that showed the expected surfaces for such a sort of non-covalent interactions (Figure 5).

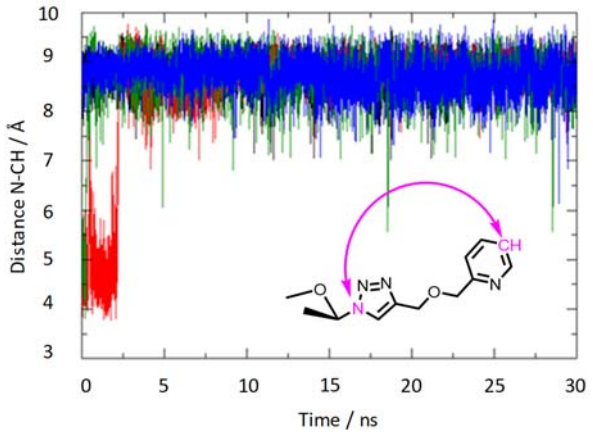

Figure 4. Molecular dynamics of **10** showing unfolding after 2.5 ns and its maintenance up to 30 ns (extension to 100 ns do not show any change). Starting structures: red trace: protonated folded; green trace: neutral folded; black trace: protonated unfolded; blue trace: neutral unfolded

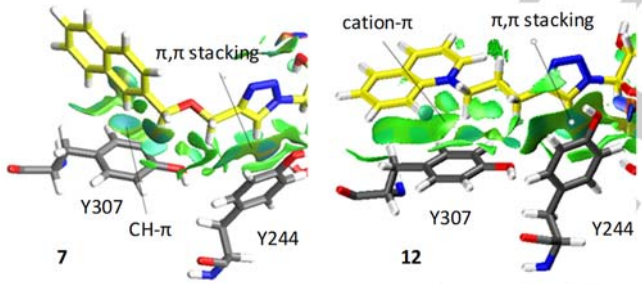

Figure 5. NCI analysis showing characteristic surfaces for T-shape (left, compound **7**) and parallel (right, compound **12**) oriented ligands corresponding to CH-π and azinium-π (cation-π) interactions, respectively.

As a final verification of our approach, we conducted inhibition studies of the best ligand **12** on *Af*Gel4.[19] The experiments indicated that this compound was capable of inhibiting *Af*Gel4 with an IC_{50} value of 42.0 μM (See SI), validating our approach of using *Sc*Gas2 as a model for the design of glycomimetics against *Af*Gel4.

In summary, after a rational design of ligands for *Af*Gel4 using *Sc*Gas2 as a model, we have obtained quinolinium derivative **12** showing a K_d of 1.50 ± 0.01 μM and inhibitory properties against *Af*Gel4 (IC_{50} = 42 μM). During the design, π,π-interactions with Tyr307 and Tyr244 were discovered to be the driving force for achieving optimal binding. In particular, in the case of Tyr244, interactions with positively charged aromatic residues favours a parallel orientation of the aromatic rings, which enhances the strength of the resulting azinium-π (cation-π) interactions. Understanding the ultimate conditions to design a good ligand for *Sc*Gas2 we obtained a first low micromolar inhibitor for *Af*Gel4 demonstrating the validity of the approach. These studies will open the door to the design of more potent inhibitors of *Af*Gel4 that could be useful as a platform to discover antifungal therapeutic agents.

Acknowledgements

This work was supported by Spanish MINECO Contracts (CTQ2016-76155-R to P.M., and BFU2016-75633-P to R.H-G.), and an MRC Programme Grant (M004139) to D.M.F.v.A. We also acknowledge the Government of Aragón (Spain) (Bioorganic Chemistry group E-10 and Protein Targets group B-89) for financial support. We acknowledge the Institute of Biocomputation and Physics of Complex Systems (BIFI) at the University of Zaragoza (Spain) for computer time at clusters Terminus and Memento. We thank synchrotron radiation sources DLS (Oxford), and in particular beamline I02 (experiment number MX10121-11), and ALBA (Barcelona), and in particular XALOC beamline. European Commission is gratefully acknowledged (BioStruct-X grant agreement N°283570 and BIOSTRUCTX_5186).

Keywords: transglycosylases • *Aspergillus fumigatus* • oligosaccharides • glycomimetics • carbohydrates

[1] I. V. Ene, L. A. Walker, M. Schiavone, K. K. Lee, H. Martin-Yken, E. Dague, N. A. Gow, C. A. Munro, A. J. Brown, *mBio* **2015**, *6*, e00986.
[2] J. P. Latge, *Mol. Microbiol.* **2007**, *66*, 279-290.
[3] (a) I. Mouyna, L. Hartl, J. P. Latge, *Frontiers in microbiology* **2013**, *4*, 81. (b) E. Cabib, J. Arroyo, *Nat. Rev. Microbiol.* **2013**, *11*, 648-655.
[4] A. Gastebois, T. Fontaine, J. P. Latge, I. Mouyna, *Eukaryot. Cell* **2010**, *9*, 1294-1298.
[5] (a) F. Sillo, C. Gissi, D. Chignoli, E. Ragni, L. Popolo, R. Balestrini, *Fungal Genet. Biol.* **2013**, *53*, 10-21. (b) W. Zhao, C. Li, J. Liang, S. Sun, *Glycobiology* **2014**, *24*, 418-427.
[6] (a) E. Ragni, A. Coluccio, E. Rolli, J. M. Rodriguez-Pena, G. Colasante, J. Arroyo, A. M. Neiman, L. Popolo, *Eukaryot. Cell* **2007**, *6*, 302-316. (b) E. Ragni, J. Calderon, U. Fascio, M. Sipiczki, W. A. Fonzi, L. Popolo, *Fungal Genet. Biol.* **2011**, *48*, 793-805. (c) M. de Medina-Redondo, Y. Arnaiz-Pita, C. Clavaud, T. Fontaine, F. del Rey, J. P. Latge, C. R. Vazquez de Aldana, *PLoS One* **2010**, *5*, e14046.
[7] R. Hurtado-Guerrero, A. W. Schuettelkopf, I. Mouyna, A. F. M. Ibrahim, S. Shepherd, T. Fontaine, J.-P. Latge, D. M. F. van Aalten, *J. Biol. Chem.* **2009**, *284*, 8461-8469.
[8] L. Raich, V. Borodkin, W. Fang, J. Castro-Lopez, D. M. F. van Aalten, R. Hurtado-Guerrero, C. Rovira, *J. Am. Chem. Soc.* **2016**, *138*, 3325-3332.
[9] I. Delso, J. Valero-González, E. Marca, T. Tejero, R. Hurtado-Guerrero, P. Merino, *Chem. Biol. Drug Design* **2016**, *87*, 163-170.
[10] J. L. Asensio, A. Arda, F. J. Canada, J. Jimenez-Barbero, *Acc. Chem. Res.* **2013**, *46*, 946-954.
[11] M. Kumar, P. V. Balaji, *J. Mol. Model.* **2014**, *20*, 2136.
[12] C. D. Hein, X. M. Liu, D. Wang, *Pharm. Res.* **2008**, *25*, 2216-2230.
[13] V. K. Tiwari, B. B. Mishra, K. B. Mishra, N. Mishra, A. S. Singh, X. Chen, *Chem. Rev.* **2016**, *116*, 3086-3240.
[14] T. Tejero, S. García-Viñuales, I. Delso, P. Merino, *Synthesis* **2016**, *48*, 3339-3351.
[15] C. R. Martinez, B. L. Iverson, *Chem. Sci.* **2012**, *3*, 2191-2201.

10.1002/cmdc.201700720

[16] S. Yamada, N. Yamamoto, E. Takamori, *J. Org. Chem.* **2016**, *81*, 11819-11830.
[17] R. Anjana, M. K. Vaishnavi, D. Sherlin, S. P. Kumar, K. Naveen, P. S. Kanth, K. Sekar, *Bioinformation* **2012**, *8*, 1220-1224.
[18] (a) E. R. Johnson, S. Keinan, P. Mori-Sanchez, J. Contreras-Garcia, A. J. Cohen, W. Yang, *J. Am. Chem. Soc.* **2010**, *132*, 6498-6506. (b) J. R. Lane, J. Contreras-Garcia, J.-P. Piquemal, B. J. Miller, H. G. Kjaergaard, *J. Chem. Theory Comput.* **2013**, *9*, 3263-3266.
[19] The biological evaluation of **12** towards *Af*Gel4 was carried out through a competition assay using a mixture of G14- and G15-laminooligosaccharides, where their disappearance was quantified by RP-UPLC.

10.1002/cmdc.201700720

WILEY-VCH

Entry for the Table of Contents (Please choose one layout)

COMMUNICATION

Structure-guided design using a transglycosylase from *Saccharomyces cerevisiae* as a model led to a micromolar inhibitor of pathogenic *Aspergillus fumigatus*

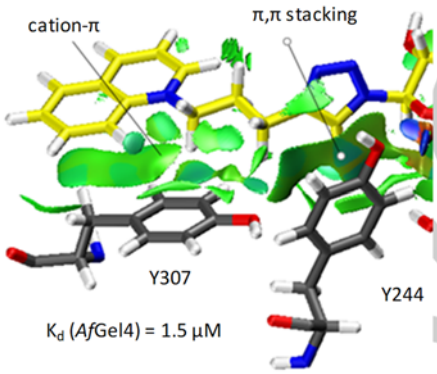

I. Delso, J. Valero-Gonzalez, F. Gomollón-Bel, J. Castro-López, W. Fang, I. Navratilova, D. M.F. van Aalten, T. Tejero, P. Merino,* and R. Hurtado-Guerrero**

Page No. – Page No.

Inhibitors against Fungal Cell Wall-remodelling Enzymes .